21

Generation and Detection of Pulsed Terahertz Radiation Using Photoconductive Semiconductor Antennas Based on LT-$In_xGa_{1-x}N$/GaN

© E.R. Burmistrov[1,2], L.P. Avakyants[1], N.A. Parfentieva[2], S.N. Gavrilin[2]

[1] Lomonosov Moscow State University, Physics Department
Moscow, Russia
[2] National Research Moscow State University of Civil Engineering,
Moscow, Russia
e-mail: burmistrover@my.msu.ru

Received June 07, 2025
Revised July 19, 2025
Accepted July 30, 2025

The generation and detection of terahertz (THz) radiation using photoconductive antennas based on low-temperature grown LT-$In_xGa_{1-x}N$/GaN heterostructures were investigated. Multilayer structures grown by metal-organic chemical vapor deposition demonstrated efficient conversion of femtosecond laser radiation into THz pulses $8 \cdot 10^{-5}$. At an optical pumping power of 57 mW and bias voltage of 15 V, an average THz radiation output power of 4.5 μW was achieved. The frequency spectrum of the emission is concentrated in the range 1.0–1.2 THz with a bandwidth up to 3 THz. Temporal and spectral characteristics of the signal were studied, as well as the dependencies of THz radiation power on pumping and bias parameters. The results confirm the prospects of using LT-$In_xGa_{1-x}N$/GaN for creating THz sources and detectors, opening new possibilities for THz spectroscopy and optoelectronics applications.

Keywords: photoconductive antennas, gallium nitride, terahertz radiation, optical pumping, temporal shapes, pulsed terahertz spectroscopy.

DOI: 10.61011/EOS.2025.09.62312.8258-25

Introduction

Recently, the terahertz (THz) frequency range (0.1–10 THz) has become one of the most important research areas in photonics and optoelectronics [1]. Special attention is focused on developing efficient methods for generating and detecting pulsed THz radiation using semiconductor materials. The interest is primarily due to these materials' ability to convert optical radiation into THz electromagnetic waves, which opens new possibilities not only for applied developments such as THz imaging but also for fundamental condensed matter physics research [2].

Photoconductive semiconductor antennas (PCAs) play a central role in pulsed THz spectroscopy. Key PCA properties include direct conversion of femtosecond laser radiation into THz waves and the inverse conversion of THz radiation into measurable electrical signals while preserving the phase and amplitude information of the original pulse. PCAs are widely used in time-resolved THz spectroscopy (THz-TDS) [2,3].

Broadband THz radiation generation is mainly implemented by several methods: (i) optical rectification in nonlinear crystals with quadratic nonlinearity [4], (ii) excitation of ultrafast photoconductivity in semiconductor electro-optical materials [5] and (iii) Cherenkov radiation in polarized ferroelectric structures with nonlinear response [6]. Despite various generation mechanisms, photoconductivity remains dominant in semiconductors [7].

When photons emitted by a femtosecond laser are absorbed in the PCA photoconductive layer, electron-hole pairs are generated. This can occur through direct absorption above the bandgap or lower energy mechanisms such as multiphoton absorption or impurity levels. Photoinduced nonequilibrium charge carriers create an electric dipole moment that screens the applied electric field. Terahertz radiation arises from a transient current induced by the rapid change in photoconductivity when femtosecond pulses are absorbed [8]. The antenna structure acts as a radiating element converting current to THz electromagnetic waves. The process efficiency depends on laser radiation parameters (wavelength, intensity), photoconductive layer properties (carrier mobility, lifetime), and antenna geometry. Notably, THz generation in PCAs can occur without an applied electric field, as observed in bias-free PCA sources that do not require external bias. A detailed study of this effect is presented in [9–11].

Electrode configuration plays a special role, significantly affecting the spatial distribution of photocurrent and, consequently, determining the spectral composition and signal-to-noise ratio of the THz emission generated by the PCA [12,13]. Linear dipole antennas, which provide broadband emission thanks to subwavelength interelectrode gaps, as well as spiral structures, are the most widespread [14,15]. Particular interest is given to butterfly-type antennas, in which the specific geometry of the electrodes allows efficient control of the polarization characteristics of the emission [16,17].

In the context of the development of THz photonics, significant efforts are directed at creating compact radiation sources with high conversion efficiency. In designing PCAs for pulsed THz generation, high dark resistance and optimal antenna geometry are of decisive importance. Among promising materials for PCAs, structures based on low-temperature (LT) grown GaAs deserve special attention. The main advantage of LT-GaAs is related to its growth features at reduced temperatures, leading to excessive arsenic (As) atom concentration, which in turn forms numerous charge carrier traps [18]. Creating various trapping centers to reduce carrier lifetime is one of the central tasks in THz PCA technology. Alongside this, LT-GaAs demonstrates exceptionally high dark resistance ($10^6 - 10^9\,\Omega$), allowing voltages above 100 V to be applied to antenna gaps of width $10 - 100\,\mu$m without the risk of semiconductor structure breakdown [19].

In the work [20], using the THz-TDS method, anisotropy of the emission characteristics depending on crystallographic orientation in LT-GaAs-based PCAs with spiral antenna type was discovered. It was shown that samples oriented along (111) exhibit fourfold superiority in the power of generated THz radiation compared to samples oriented along (100).

Particular interest lies in generating THz radiation using PCAs based on LT-$In_xGa_{1-x}As$. The narrow bandgap, the magnitude of which is determined by the indium (In) concentration, provides high material sensitivity to visible and infrared (IR) radiation. This property becomes especially significant when used in systems with Ti:Sa lasers. The work [21] demonstrated the possibility of broadband THz generation under optical excitation of beryllium (Be)-doped PCA based on LT-$In_xGa_{1-x}As$ by laser radiation with a wavelength of $1.56\,\mu$m. Spectral measurements showed that the upper limit of generated THz radiation reaches 3 THz.

In modern pulsed THz spectroscopy systems, the key parameters determining the efficiency of PCA detectors are high carrier mobility and short carrier lifetime. It has been experimentally established that high mobility ensures rapid PCA response to THz electromagnetic fields due to effective separation of induced carriers. Simultaneously, a short carrier lifetime (< 1 ps) allows extending the detectable frequency range and increasing the signal-to-noise ratio. In particular, studies of standard LT-GaAs structures with „butterfly“ antenna configuration showed that with mobility $400\,cm^2 \cdot V^{-1} \cdot s^{-1}$ and carrier lifetime 0.5 ps, the upper detectable frequency limit is 3 THz [22].

Using PCA sources based on superlattice structures allows a significant increase in optical-to-THz signal conversion efficiency due to increased photoconductivity. Measurements showed that at the same pumping power, superlattice PCA sources based on LT-InGaAs/InAlAs demonstrate THz signal amplitude 2–3 times higher than traditional LT-GaAs [20] antennas. In studies of PCAs based on InAs/GaAs, carrier mobilities of $843\,cm^2 \cdot V^{-1} \cdot s^{-1}$ were achieved while maintaining carrier lifetimes of 1.2 ps [23]. Further PCA technology development is associated with the use of heterostructures based on InGaAs/InAlAs superlattices, which allowed not only a substantial increase in THz pulse amplitude but also an expansion of the working bandwidth up to 4 THz [24].

Particular interest is represented by studies [25,26] demonstrating THz radiation generation in InGaN/GaN heterostructures with multiple quantum wells (MQWs). Experimental results and theoretical modeling allowed establishing that in such structures, the generation mechanism is associated with dynamic polarization processes in the active region. In particular, it was shown that photoexcited electron-hole pairs cause nonstationary screening of the built-in electric field.

Studies of GaN crystals grown at low temperatures revealed unique characteristics including a wide bandgap (3.5 eV), low dark current, and high mobility of main charge carriers ($\sim 10^3\,cm^2 \cdot V^{-1} \cdot s^{-1}$) [6]. The low-temperature growth process ($T < 500\,^\circ$C) leads to the incorporation of excess N_2 atoms into the GaN lattice, formation of nitrogen vacancies, and emergence of deep energy levels in the bandgap. As a consequence, the lifetime of main charge carriers is significantly reduced, reaching values of $\sim 10^{-12}$ s. The work [27] using THz-TDS analyzed optical and electrophysical properties of $In_xGa_{1-x}N$ films with In content from 7% to 14% in the frequency range $0.3 - 3$ THz. It was found that the refractive index and conductivity of $In_xGa_{1-x}N$ monotonically increase with In content, reaching maximum values for InN. It was revealed that at In concentration above 10%, significant effects of defects and heterogeneities in the semiconductor structure appear.

Thus, LT-$In_xGa_{1-x}N$/GaN heterostructures with increased In content ($> 20\,\%$) in the photoconductive layer represent a promising class of materials for PCAs with a number of advantages compared to traditionally used LT-GaAs and LT-$In_xGa_{1-x}As$. This work experimentally demonstrates for the first time the possibility of creating and using PCAs based on LT-$In_xGa_{1-x}N$/GaN superlattices, opening new prospects for the development of THz electronic devices.

Experimental samples of photoconductive THz antennas based on LT-$In_xGa_{1-x}N$/GaN

This section presents research results on generation and detection of THz pulses using PCAs based on LT-$In_xGa_{1-x}N$/GaN superlattice structures. The studied heterostructures were grown by metal-organic chemical vapor deposition (MOCVD). Samples from manufacturer AO „Svetlana-Rost“ were investigated. Figure 1 shows a schematic and the layer structure of the investigated PCAs.

On a sapphire substrate with crystallographic orientation (0001), a multilayer structure was grown. Initially, a LT-AlN buffer layer of 100 nm thickness was formed to reduce lattice mismatch between the substrate and subsequent layers. Then, a 50 nm thick AlGaN intermediate layer was deposited, serving as a charge carrier barrier. The

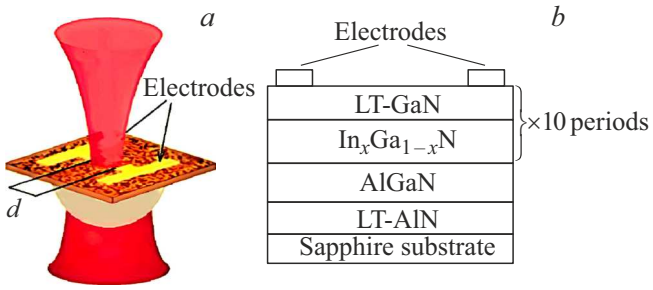

Figure 1. External view (a) and layer structure (b) of PCA based on LT-$In_xGa_{1-x}N$/GaN, with indicated interelectrode gap d.

active region of the structure consisted of 10 periods of $In_xGa_{1-x}N$/GaN layers with thicknesses of 5 nm and 15 nm respectively, where In content was 32%. All layers were grown at a reduced temperature of 450 °C. The capping LT-GaN layer also served to protect against surface breakdown. The total thickness of the photoconductive layer was 200 nm.

After growth, the structure underwent thermal treatment involving rapid annealing at 450 °C for 1 minute in a nitrogen N_2 atmosphere with subsequent controlled cooling at a rate of 10 °C/s. This procedure contributed to mechanical stress relaxation and improvement of the electrical properties of the PCA. Annealing modes were specifically optimized considering the requirements for THz antennas, where low contact resistance and high carrier mobility in contact areas are critically important.

To create the dipole antenna structure, ohmic contacts were formed characterized by linear current-voltage (I-V) characteristics and low barrier potential. The gap between electrodes was 10 μm. A multilayer Ti/Al/Ni/Au system with a thickness of 300 nm was deposited by thermal evaporation. Titanium provided adhesion to the semiconductor surface. Aluminum was used as the main conductive channel. Nickel prevented mutual diffusion of charge carriers, and gold coating protected the surface from oxidation.

Note that compared to single-layer structures, multilayer ones possess better electrical and optical properties due to heterointerface effects, such as roughness, which facilitate charge carrier transport in the active region. Thanks to deep defect levels in these structures, picosecond carrier lifetimes can be achieved, significantly reducing the scattering rate of photoexcited carriers, which in turn is accompanied by a reduction in relaxation time and dark current.

During THz radiation generation, the PCA electrodes were connected to a power supply (Fig. 2). The current pulse J, created during the absorption of femtosecond laser pulses in the PCA is directly proportional to the external electric field strength generated by the DC source:

$$J = \langle N \rangle e \mu E_{DC} \tag{1}$$

where $\langle N \rangle$ is the average concentration of photoexcited carriers, $E_{DC} = U_{DC}/d$ is the external electric field strength,, U_{DC} is the bias voltage of the external source. For THz pulse registration, PCA electrodes were connected to a highly sensitive current meter ($\sim 10^{-16}$ A). The detection current was formed by the simultaneous interaction of femtosecond and THz pulses in the interelectrode gap on the PCA surface. If the THz pulse electric field strength is E_{THz}then the resulting current pulse is $J \sim E_{\mathrm{THz}}$. The laser pulse duration is much shorter than the period of THz electromagnetic wave oscillations.

The THz pulse electric field generated by PCA can be described in the dipole radiation approximation without considering the specific type of carrier oscillatory relaxation by the following expression:

$$E_{\mathrm{THz}} = \frac{Ae}{4\pi\varepsilon_0 c^2 r} \frac{\partial N(t)}{\partial t} \mu U_{DC} \tag{2}$$

where A is the spot area in the electrode gap, $N(t)$ is the time-dependent photoexcited carrier concentration with mobility μ, r is the distance from PCA to the spatial point where the electric field strength of the THz electromagnetic wave is to be calculated. The relation (2) assumes the distance between PCA and any space point for THz field calculation exceeds the PCA size.

Experimental procedure

Our research group developed an experimental setup to study the spectral characteristics of PCAs based on LT-$In_xGa_{1-x}N$/GaN structure, implementing the standard THz-TDS scheme. This methodology proved effective earlier in the work [28] and was successfully applied to plasmonic detection of THz radiation in multilayer semiconductor heterostructures InGaN/AlGaN/GaN. The experimental setup schematic is shown in Fig. 2.

The setup included a Ti:Sa laser ($\lambda = 800$ nm, wavelength, pulse duration 130 fs, average output power 57 mW, repetition rate 60 MHz). Beam splitter (Beamsplitter 1) split the beam with diameter 1.8 mm into pump and reference beams, which traveled different optical paths. The pump beam was used in the THz impulse generation channel in PCA1 (Photoconducting switch 1). The reference beam passed through an optical delay line (Delay stage) formed by mirrors 4–7 (Mirrors 4–7) and was used in the coherent detection scheme. Synchronization of pulse arrival times at PCA2 detector (Photoconducting switch 2) was achieved by adjusting the distance between Mirror 4 and Mirror 5. The detector antenna PCA2 was identical to PCA1 emitter. In detector mode, electrical current in PCA2 is proportional to the instantaneous electric field strength of THz pulses.

Since the Ti:Sa laser generates radiation at 800 nm wavelength, the photon energy is 1.55 eV. As noted earlier, one key advantage of PCAs based on LT-$In_xGa_{1-x}N$/GaN structures is their wide bandgap (~ 3.4 eV). Electron transition from valence to conduction band requires energy exceeding the bandgap. In three-photon absorption, the total energy

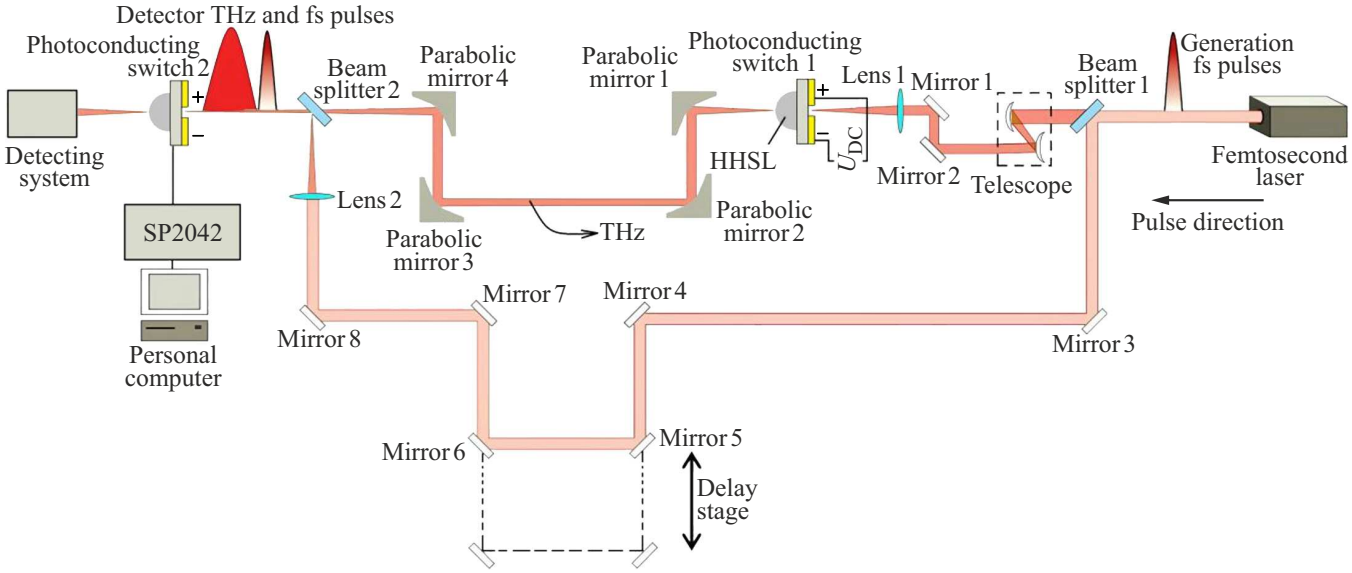

Figure 2. Schematic of the THz-TDS experimental setup.

of three photons (4.65 eV) is sufficient for photoexcitation, but this process has low probability and requires high laser intensity, making it energetically inefficient.

Charge carriers in PCAs based on LT-$In_xGa_{1-x}N$/GaN were excited using the second harmonic of Ti:Sa laser at 400 nm wavelength (photon energy 3.1 eV). Features of the wurtzite GaN crystal structure with hexagonal symmetry grown along the polar direction (0001) lead to built-in electric fields at the $In_xGa_{1-x}N$/GaN heterointerface with strengths up to MV/m caused by spontaneous and piezoelectric polarizations. These fields, due to GaN's polar nature, play an important role in the THz generation mechanism by enabling efficient carrier separation immediately after photoexcitation. During dynamic screening of built-in fields, picosecond current pulses form. This process is mathematically described by the displacement current equation:

$$P(t) \propto \int_0^t J_{\text{bias}}(t')dt', \qquad (3)$$

where J_{bias} is the polarization-related displacement current, t is the duration of the femtosecond pulse.

To correctly study PCAs properties based on LT-$In_xGa_{1-x}N$/GaN it was necessary to suppress this „spurious" generation. Experimental conditions were selected to neutralize the contribution of dynamic screening of built-in fields. This was achieved by applying an external field of opposite polarity relative to the internal field. The pump beam incident on PCA1 at the Brewster angle had P-polarization of the electric field. At the Brewster angle, maximum P-polarized light energy enters the material, minimizing reflection. The femtosecond laser spot size in the interelectrode gap on PCA1 surface was 4 μm allowing high spatial localization of excitation. The spot size was close to the diffraction limit, important for coherent excitation. For normal focusing lenses, the minimal spot size achievable is 5.1 μm.

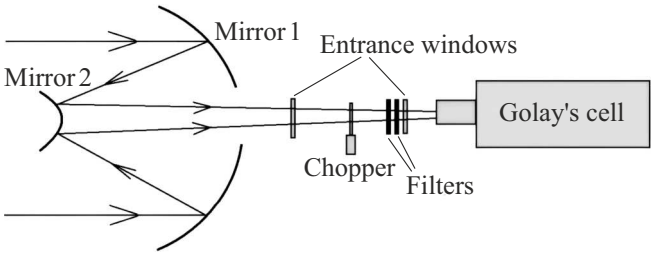

Figure 3. Schematic of the detecting system using a Golay cell.

On the substrate side, the diverging THz emission was focused by a hyper-hemispherical high-resistivity silicon lens (HHSL) with a diameter of 15 mm and directed to PCA2 detector. Detection of current pulses generated by PCA2 was conducted using synchronous amplifier SP2042 with simultaneous illumination of the gap between electrodes by THz and femtosecond pulses.

THz radiation power measurements were carried out using an optoacoustic transducer — a Golay cell. The optical input system consisted of a telescopic scheme based on two spherical mirrors providing efficient focusing of the THz beam on the detector input window with minimal energy loss due to scattering (Fig. 3).

A set of high-frequency cut-off filters was placed before the detector for spectral selection of radiation. Signal modulation was done with a mechanical chopper. Xenon was used as the working medium in the Golay cell. Terahertz radiation was absorbed by a semi-transparent plate at the device entrance, causing gas heating. On the

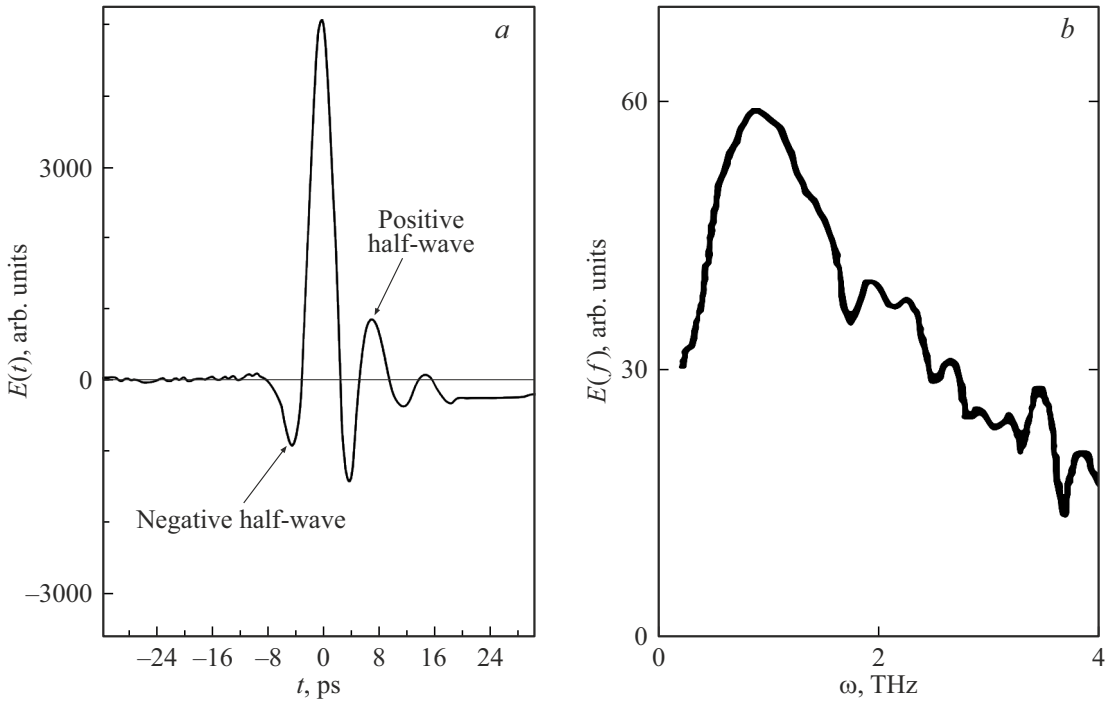

Figure 4. Temporal waveform (a) and frequency spectrum (b) of the Fourier amplitude of the THz pulse generated by a photoconductive antenna based on LT-$In_xGa_{1-x}N$/GaN.

opposite side of the chamber, there was a flexible membrane whose rear surface reflected the incident LED beam. Upon gas heating, the membrane surface bent, changing the intensity of light reflected from its rear surface, thus enabling measurement of THz radiation power.

Hall mobility and concentration of photoexcited charge carriers in PCAs based on LT-$In_xGa_{1-x}N$/GaN were determined in Van der Pauw geometry using the „EcopiaHMS-3000“ setup in magnetic fields up to 3 T in darkness at room temperature.

Experimental results

As seen in Fig. 4, the presented experimental data demonstrate the temporal and spectral characteristics of THz radiation generated by PCA based on LT-$In_xGa_{1-x}N$/GaN. When analyzing PCA operation, the key parameter is not the absolute bias voltage but the electric field strength $E = U_{DC}/d$, defined as the ratio of the external source voltage U_{DC} to the electrode gap distance d. In the studied PCAs with 10 μm interelectrode gaps at 15 V bias, an electric field strength of 1.5 MV/m is created.

The recorded single-cycle signal clearly exhibits positive and negative half-waves. Fig. 4, b shows the noise component in the high-frequency region manifesting as a characteristic „tail“.

From Fig. 4, a it can be seen that the full width at half maximum of the main peak is approximately 4000 fs. The step of the controlled optical delay line in the experimental setup is 5 μm corresponding to 17 fs. Thus, the temporal profile of the THz pulse was obtained by accumulating a sample of field strength values comprising 235 points.

Hall effect measurements showed that in the PCA based on LT-$In_xGa_{1-x}N$/GaN the mobility and concentration of majority charge carriers are $\mu_H = 170\,\mathrm{cm}^2 \cdot \mathrm{V}^{-1} \cdot \mathrm{s}^{-1}$ and $n_H = 5.2 \cdot 10^{12}\,\mathrm{cm}^{-2}$ respectively. The dark resistance of the photoconductive layer was 90 MΩ.

Based on well-known trends, the effective mass of two-dimensional carriers in the $In_xGa_{1-x}N$ solid solution should be smaller than that in binary GaN, for which both experimental data and first-principle theoretical calculations give values in the range $0.18 - 0.24m_0$ (where m_0 is the free electron mass). Direct measurements of the electron effective mass in $In_xGa_{1-x}N$ ($x = 20\,\%$) considering composition fluctuations yield values in the range $0.194 - 0.197m_0$ [29]. For narrower bandgap quantum wells $In_xGa_{1-x}N$ ($x = 33\,\%$) the authors of work [30] report values $0.204 - 0.205m_0$. The estimate of the lifetime of photoexcited carriers in PCAs based on LT-$In_xGa_{1-x}N$/GaN using the relation $\tau = \mu m^*/e$ gives a value of 200 ps. The bandwidth of the PCA based on LT-$In_xGa_{1-x}N$/GaN was approximately 3 THz.

It should be noted that although the reduction of carrier lifetime in PCAs leads to the broadening of their frequency response (which mathematically follows from the Fourier transform), the actual operational bandwidth of a THz spectrometer is primarily determined by the matched operation of the entire „source-detector“ system. If the detector has a significantly longer carrier lifetime, its frequency response becomes a limiting factor. In this case, reducing τ in the

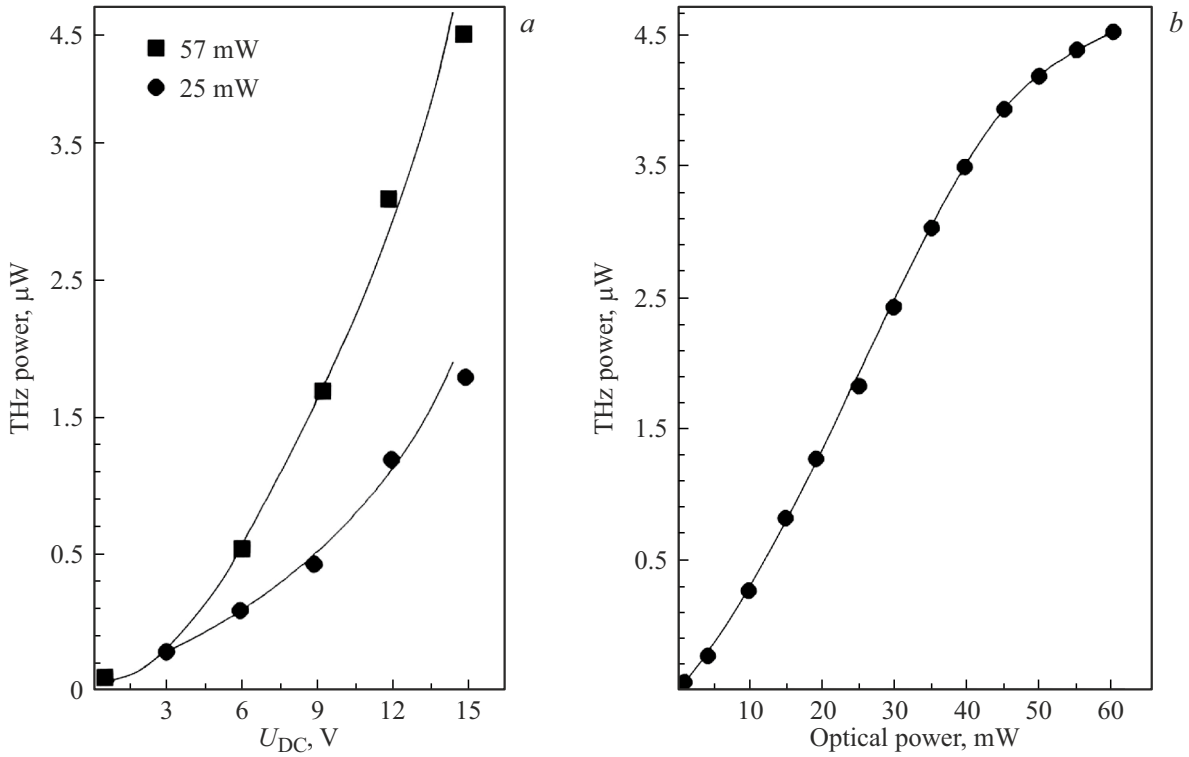

Figure 5. Dependence of THz radiation power of the antenna based on LT-$In_xGa_{1-x}N$/GaN on bias voltage (*a*) and optical pumping power (*b*) at bias voltage 15 V.

source will not lead to a significant expansion of the overall system bandwidth. Optimal spectrometer operation requires matching the temporal parameters of both components.

Fig. 5 shows experimentally obtained dependencies of THz radiation power of the PCA based on LT-$In_xGa_{1-x}N$/GaN on applied bias voltage and average femtosecond laser radiation.

A comparative analysis of efficiencies of various PCAs showed the following. In [31], for a PCA based on LT-GaAsc with dipole topology, at optical pumping power $P_{pomp} = 15\,\text{mW}$ and bias voltage $U_{DC} = 30\,\text{V}$ a THz radiation power of $P_{\text{THz}} = 0.34\,\mu\text{W}$ was registered. Extrapolation of these data in the linear regime (assuming no saturation or thermal degradation) for $P_{pomp} = 57\,\text{mW}$ gives an expected value of $P_{\text{THz}} = 4.9\,\mu\text{W}$. The characteristic efficiency figure amounts to $\eta = 8.6 \cdot 10^{-5}$. However, experimental data indicate a substantial deviation from the linear dependence at high pumping levels. The observed saturation effect, caused by screening of the applied electric field by photocarriers, results in reduced output THz power. As a result, the real power does not reach the theoretically predicted $4.9\,\mu\text{W}$.

Higher THz conversion efficiency ($\eta = 1.2 \cdot 10^{-4}$) was achieved in PCAs based on Si-GaAs [22], where at $P_{pomp} = 19\,\text{mW}$ and $U_{DC} = 30\,\text{V}$ $P_{\text{THz}} = 2.3\,\mu\text{W}$ was obtained. Similar studies [32] at $P_{pomp} = 20\,\text{mW}$ and $U_{DC} = 20\,\text{V}$ demonstrate values P_{THz} in the range $1 - 2\,\mu\text{W}$, which agrees with results for PCAs based on InGaAs [9–11]. In our experiments with PCAs based on LT-$In_xGa_{1-x}N$/GaN using a Golay cell, a THz radiation power$P_{\text{THz}} = 4.5\,\mu\text{W}$ was achieved at optical pump power $P_{pomp} = 57\,\text{mW}$ with conversion efficiency $\eta = 8 \cdot 10^{-5}$.

Analysis of experimental curves revealed a superlinear nature of the dependence of THz radiation power on the applied bias voltage in the range $0 - 15\,\text{V}$. The obtained dependence is accurately described by the theoretical function $W \sim U_{DC}^b$, where at optical pump powers of 57 and 25 mW, the exponent b takes values 1.8 and 1.5, respectively. The dependence of THz radiation power on optical pump power also demonstrates a superlinear form.

One key factor determining the efficiency of THz radiation generation in the studied PCAs based on LT-$In_xGa_{1-x}N$/GaN is the impact ionization process occurring at high electric fields ($> 10^5\,\text{V/m}$). The obtained superlinear dependencies of THz power on bias voltage and optical pump power indicate a significant contribution of this process to photocurrent formation. At threshold electric field strength values (1.5 MV/m in our experiments), photoinduced carriers acquire sufficient energy for lattice atom ionization upon collisions, leading to avalanche-like growth in free carrier concentration and signal saturation at high pump levels (above $\sim 50\,\text{mW}$) [22].

Spectral characteristic analysis showed that this mechanism does not significantly degrade the temporal resolution of the entire system since carrier lifetime in the studied PCAs remains at $\sim 200\,\text{ps}$. However, at further increased

field strength above 2 MV/m, the noise component in the spectrum grows, possibly related to instability development in the avalanche ionization process.

These results suggest that further optimization of the composition of $In_xGa_{1-x}N/GaN$ (particularly increasing In content in the range $x = 0.4 - 0.5$) may reduce the threshold for impact ionization by decreasing the effective carrier mass, which is of great interest for creating more efficient PCA THz generators. At the same time, possible degradation of crystalline quality at high In concentrations must be considered, requiring careful growth conditions adjustment.

Conclusion

This work studied the processes of pulsed THz generation and detection using PCAs based on low-temperature heterostructures LT-$In_xGa_{1-x}N/GaN$. The main research results can be summarized as follows.

It was experimentally established that developed multilayer structures grown by metal-organic chemical vapor deposition containing 10 periods of $In_xGa_{1-x}N/GaN$ with Indium molar fraction $x = 0.32$ demonstrated efficient conversion of femtosecond laser radiation into THz pulses $8 \cdot 10^{-5}$ at optical pump power 57 mW and bias voltage 15 V. An average THz output power of 4.5 μW was achieved.

Spectral analysis using THz-TDS showed that the emission peak of the PCA lies in the range $1.0 - 1.2$ THz with a bandwidth up to 3 THz. Temporal signal measurements revealed a THz pulse duration of about 4 ps, consistent with measured carrier lifetime (~ 200 ps) and mobility ($\sim 170\,cm^2 \cdot V^{-1} \cdot s^{-1}$).

Special attention was given to the study of dependencies of THz power on excitation parameters. It was found that the dependence on bias voltage is superlinear, indicating the role of impact ionization processes at high fields. Observed saturation of output signal at pump powers above 50 mW is explained by electric field screening by photoinduced carriers.

This work contributes to semiconductor physics and THz generation, serving as a step toward more efficient THz sources and detectors. The results are important for the development of pulsed THz spectroscopy methods, as the developed PCAs can be used as compact THz emission sources and detectors for various spectroscopic studies.

Acknowledgments

The authors express gratitude to Prof., Dr. of Physical and Mathematical Sciences G.Kh. Kitaeva for the idea of this work.

Funding

The work was supported by a 2025 fundamental scientific research grant (NIR/NIOR) by scientific teams of NRU MGSU, project No. 15-661/130, and the Foundation for Theoretical Physics and Mathematics Development „Basis“.

Conflict of interest

The authors declare that they have no conflict of interest.

References

[1] A. Krotkus. J. Phys. D, **43** (27), 273001 (2010). DOI: 10.1088/0022-3727/43/27/273001
[2] N.M. Burford, M.O. El-Shenawee. Opt.Engineer., **56** (1), 010901 (2017). DOI: 10.1117/1.OE.56.1.010901
[3] D. Pashnev, T. Kaplas, V.V. Korotyeyev, K.M. Borysenko, S.A. Vitusevich. Appl.Phys.Lett., **117** (5), 051105 (2020). DOI: 10.1063/5.0014977
[4] S.H. Yang, M.R. Hashemi, C.W. Berry, M. Jarrahi. IEEE Trans. Terahertz Sci. Technol., **4** (5), 575 (2014). DOI: 10.1109/TTHZ.2014.2342505
[5] D.H. Auston, K.P. Cheung, P.R. Smith. Appl.Phys.Lett., **45** (3), 284 (1984). DOI: 10.1063/1.95174
[6] D.H. Auston, K.P. Cheung, J.A. Valdmanis, D.A. Kleinman. Phys. Rev. Lett., **53** (16), 1555 (1984). DOI: 10.1103/PhysRevLett.53.1555
[7] O. Imafuji, B.P. Singh, Y. Hirose, Y. Fukushima, S. Takigawa. Appl. Phys. Lett., **91** (7), 071112 (2007). DOI: 10.1063/1.2771528
[8] D.H. Auston. Appl. Phys. Lett., 26 (3), 101 (1975). DOI: 10.1063/1.88079
[9] D.S. Ponomarev, R.A. Khabibullin, A.E. Yachmenev, A.Yu. Pavlov, D.N. Slapovskiy, I.A. Glinskiy, D.V. Lavrukhin, O.A. Ruban, P.P. Maltsev. Semiconductors, **51** (9), 1267 (2017). DOI: 10.21883/FTP.2017.09.44893.8508
[10] D.V. Lavrukhin, Yu.G. Goncharov, P.A. Khabibullin, K.I. Zaytsev, D.S. Ponomarev. Techn. Phys. Lett., **50** (8), 368 (2024). DOI: 10.61011/PJTF.2024.08.57513.19839
[11] D. Turan, N.T. Yardimci, P.K. Lu, M. Jarrahi. In: *International Microwave Symposium* (IEEE/MTT-S, 2020), p. 87. DOI: 10.1109/IMS30576.2020.9224081
[12] V. Adhikar, A. Karmakar, B. Biswas, C. Saha. In: *Advances in Terahertz Technology and its Applications* (Springer, Singapore, 2021), p. 1. DOI: 10.1007/978-981-16-5731-3_1
[13] N. Sharma, A. Kaur. In: *World Conference on Applied Intelligence and Computing* (IEEE, 2023), p. 491. DOI: 10.1109/AIC57670.2023.10263844
[14] Y. He, Y. Chen, L. Zhang, S. Wong, Z. Chen. China Commun., **17** (7), 124 (2020). DOI: 10.23919/J.CC.2020.07.011
[15] K. Demir, M. Ünlü, H. Altan, A.B. Şahin, K. Elmabruk. J. Infrared, Millimeter, and Terahertz Waves, **40** (6), 228 (2019). DOI: 10.1007/s10762-019-00588-y
[16] Y. Shi, X. Zhang, Q. Qiu, Y. Gao, Z. Huang. IEEE Access, **9**, 113823(2021). DOI: 10.1109/ACCESS.2021.3103205
[17] M.F. Ali, S. Sahu, R. Singh, G. Varshney. J. Opt., **26** (12), 125601(2024). DOI: 10.1088/2040-8986/ad8583
[18] M. Tani, K.S. Lee, X.C. Zhang. Appl.Phys.Lett., **77** (9), 1396 (2000). DOI: 10.1063/1.1289914
[19] A.M. Buryakov, M.S. Ivanov, S.A. Nomoev, D.I. Khusyainov, E.D. Mishina, V.A. Khomchenko. Mater. Res. Bull., **122**, 110688(2020). DOI: 10.1016/j.materresbull.2019.110688

[20] E. Klimov, A. Klochkov, P. Solyankin, S. Pushkarev, G. Galiev, N. Yuzeeva, A. Shkurinov. Int. J. Mod. Phys. B, **38** (28), 2450378 (2024). DOI: 10.1142/S0217979224503788
[21] A. Takazato, M. Kamakura, T. Matsui, J. Kitagawa. Appl. Phys. Lett., **91** (1), 011102 (2007). DOI: 10.1063/1.2754370
[22] LND Rosa, K.J. Alaba, N.I. Cabello, R. Loberternos, J.P. Ferrolino, I.C. Verona, V.P. Juguilon. Opt. Mater., **150**, 115212(2024). DOI: 10.1016/j.optmat.2024.115212
[23] R. Chen, X. Li, H. Du, J. Yan, C. Kong, G. Liu, G. Lu, X. Zhang, S. Song, X. Zhang, L. Liu. Nanomaterials, **14** (3), 294(2024). DOI: 10.3390/nano14030294
[24] RJB Dietz, H. Roehle, D. Stanze, V. Montanaro, H.J. Hensel, M. Schell, B. Sartorius. In: *35th International Conference on Infrared, Millimeter, and Terahertz Waves* (IEEE, 2010), p. 1 DOI: 10.1109/ICIMW.2010.5612633
[25] G. Xu, G. Sun, Y.J. Ding, I.B. Zotova, K.C. Mandal, A. Mertiri, G. Pabst, R. Roy, N.C. Fernelius. IEEE J. Selected Topics in Quant. Electron., **17**, 30(2010). DOI: 10.1109/JSTQE.2010.2046628
[26] M.F. Saleem, G.A. Ashraf, M.F. Iqbal, R. Khan, M. Javid, T. Wang. Int. J. Opt., **2023** (1), 5619799(2023). DOI: 10.1155/2023/5619799
[27] A. Gauthier-Brun, J.H. Teng, E. Dogheche, W. Liu. Appl. Phys. Lett., **100** (7), 071913 (2012). DOI: 10.1063/1.3684836
[28] E.R. Burmistrov, L.P. Avakyants. ZhETF, **163** (5), 669 (2023) (in Russian). DOI: 10.31857/S0044451023050061
[29] A. Eljarrat, L. López-Conesa, C. Magén, N. García-Lepetit, Ž. Gačević, E. Calleja, F. Peiró. Phys. Chem. Chem. Phys., **18** (33), 23264(2016). DOI: 10.1039/C6CP04493J
[30] N. Armakavicius, V. Stanishev, S. Knight, P. Kühne. Appl. Phys. Lett., **112** (8), 082103 (2018). DOI: 10.1063/1.5018247
[31] M. Tani, S. Matsuura, K. Sakai, S. Nakashima. Appl.Opt., **36** (30), 7853(1997). DOI: 10.1364/AO.36.007853
[32] N.M. Burford, M.O. El-Shenawee. Opt.Engineer., **56** (1), 010901 (2017). DOI: 10.1117/1.OE.56.1.010901

Translated by J.Savelyeva